This is a repository copy of *Unusual 1-3 peptidoglycan cross-links in Acetobacteraceae are made by L,D-transpeptidases with a catalytic domain distantly related to YkuD domains*.

White Rose Research Online URL for this paper:
https://eprints.whiterose.ac.uk/209120/

Version: Published Version

Unusual 1-3 peptidoglycan cross-links in *Acetobacteraceae* are made by L,D-transpeptidases with a catalytic domain distantly related to YkuD domains

Marcel G. Alamán-Zárate[1,‡], Brooks J. Rady[1,‡], Caroline A. Evans[2], Brooke Pian[3], Darren Greetham[1], Sabrina Marecos-Ortiz[3], Mark J. Dickman[2], Ian D. E. A. Lidbury[1], Andrew L. Lovering[4], Buz M. Barstow[3], and Stéphane Mesnage[1,*]

From the [1]Molecular Microbiology, Biochemistry to Disease, School of Biosciences, and [2]Department of Chemical and Biological Engineering, ChELSI Institute, University of Sheffield, Sheffield, UK; [3]Department of Biological and Environmental Engineering, Cornell University, Ithaca, USA; [4]School of Biosciences, University of Birmingham, Birmingham, UK

Reviewed by members of the JBC Editorial Board. Edited by Chris Whitfield

Peptidoglycan is an essential component of the bacterial cell envelope that contains glycan chains substituted by short peptide stems. Peptide stems are polymerized by D,D-transpeptidases, which make bonds between the amino acid in position four of a donor stem and the third residue of an acceptor stem (4-3 cross-links). Some bacterial peptidoglycans also contain 3-3 cross-links that are formed by another class of enzymes called L,D-transpeptidases which contain a YkuD catalytic domain. In this work, we investigate the formation of unusual bacterial 1-3 peptidoglycan cross-links. We describe a version of the PGFinder software that can identify 1-3 cross-links and report the high-resolution peptidoglycan structure of *Gluconobacter oxydans* (a model organism within the *Acetobacteraceae* family). We reveal that *G. oxydans* peptidoglycan contains peptide stems made of a single alanine as well as several dipeptide stems with unusual amino acids at their C-terminus. Using a bioinformatics approach, we identified a *G. oxydans* mutant from a transposon library with a drastic reduction in 1-3 cross-links. Through complementation experiments in *G. oxydans* and recombinant protein production in a heterologous host, we identify an L,D-transpeptidase enzyme with a domain distantly related to the YkuD domain responsible for these non-canonical reactions. This work revisits the enzymatic capabilities of L,D-transpeptidases, a versatile family of enzymes that play a key role in bacterial peptidoglycan remodelling.

Peptidoglycan is an essential component of the bacterial cell envelope that confers cell shape and resistance to a high internal osmotic pressure (1). This bag-shaped macromolecule surrounding the cytoplasmic membrane is made of disaccharide-peptides as building blocks. Their polymerization forms glycan chains alternating *N*-acetylglucosamine and *N*-acetylmuramic acid (MurNAc) residues, substituted by short pentapeptide stems containing L- and D-amino acids (2).

Depending on the bacterial species considered, the composition of peptidoglycan building blocks can vary (2), but in most bacteria (including *Escherichia coli*), pentapeptide stems are made of the sequence L-Ala-isoD-Glu-*meso*-DAP-D-Ala-D-Ala, (where DAP is diaminopimelic acid).

The polymerization of peptidoglycan has been extensively studied since the late 1950s, when it was discovered that this process is inhibited by penicillin, a beta-lactam antibiotic widely used to combat infections (3, 4). The ubiquitous enzymes that polymerize peptidoglycan, D,D-transpeptidases, are also called Penicillin Binding Proteins (PBPs). They recognize the C-terminal D-Ala-D-Ala extremity of a donor peptide stem, form an acyl-enzyme intermediate with the amino acid in position 4, and link this residue to the side-chain amino group of the amino acid in position three of an acceptor stem (4-3 cross-link). Beta-lactams are structural analogs of the D-Ala-D-Ala stems and can be used as suicide substrates (5), leading to growth arrest and cell death (6). Alternative 3-3 peptidoglycan cross-links were originally described in *Mycobacteria* (7). These types of bonds are prevalent in the peptidoglycan of important pathogens such as *Mycobacterium tuberculosis* (8), *Mycobacterium leprae* (9) and *Clostridium difficile* (10). In *Enterococcus faecium*, resistance to beta-lactams and glycopeptides can emerge when 4-3 cross-links are replaced by 3-3 cross-links. The complete bypass of the D,D-transpeptidation pathway in *E. faecium* led to the identification of the enzyme catalysing the formation of 3-3 bonds (11) which is an L,D-transpeptidase. Instead of recognizing the D-Ala-D-Ala extremity of the pentapeptide donor stem, L,D-transpeptidases use a tetrapeptide stem as a substrate. These enzymes can perform several activities depending on the substrate they use as an acceptor. They can act as a carboxypeptidase (cleaving the fourth residue of the donor stem) (12), as a transpeptidase (forming 3-3 cross-linked muropeptides or covalently anchoring proteins to peptidoglycan) (13, 14), or as an endopeptidase (cleaving 3-3 cross-links or the link between peptidoglycan and covalently attached proteins) (15–17). Finally, L,D-transpeptidases can also exchange the fourth amino acid of a peptide stem for another amino acid (18, 19).

1-3 peptidoglycan cross-links in Acetobacteraceae

The peptidoglycan structural changes catalyzed by L,D-transpeptidases (called remodeling) play an important role in cell shape (12), resistance to abiotic stress (20), pathogenesis, and host immunity (21). All L,D-transpeptidases described to date contain a YkuD (Pfam: PF03734)) domain.

A recent study described the existence of peptidoglycan 1-3 cross-links in *Acetobacteraceae* and proposed that this unusual type of cross-link could play a role in the survival of these organisms in the context of their interaction with the fly immune system and during competition with other organisms (22). In this work, we describe a version of the PGFinder software that can automate the analysis of peptidoglycans with 1-3 cross-links. Using this tool, we determine the high-resolution structure of *Gluconobacter oxydans* peptidoglycan and reveal that it contains a high proportion of previously undescribed disaccharide-dipeptides with non-canonical amino acids at their C-terminus. Using a transposon mutant and its complemented derivative, as well as heterologous expression experiments, we demonstrate that *G. oxydans* 1-3 cross-links are formed by an enzyme with a domain distantly related to the YkuD domain of canonical L,D-transpeptidases. Collectively, our data show that L,D-transpeptidases have evolved to carry out enzymatic reactions using either tetrapeptide or dipeptide stems as donors.

Results

Building a software tool for the structural analysis of 1-3 cross-linked peptidoglycans

Prior to this study, the PGFinder software (v1.0.3; https://mesnage-org.github.io/pgfinder/) could only generate dimers and trimers crosslinked *via* 3-3 and 4-3 bonds (23). To perform the structural analysis of *G. oxydans* peptidoglycan, we modified PGFinder and its graphical user interface to enable the creation of dynamic databases containing dimers and trimers with 1-3 cross-links. This upgrade (v1.1.0) was tested using datasets from *G. oxydans*.

High-resolution analysis of G. oxydans B58 peptidoglycan

Peptidoglycan was purified from *G. oxydans* B58 cells harvested during both exponential (Fig. 1A) and stationary phase (Fig. 1B). As expected, the muropeptide profiles revealed changes indicative of major peptidoglycan remodeling during the stationary phase. We used a combination of automated tools previously described to determine the high-resolution structure of *G. oxydans* peptidoglycan (18, 23). A two-step custom search strategy was followed (Fig. S1). We first used the proprietary Byonic software to identify monomers based on tandem mass spectrometry data. The search space contained mono-, di-, tri-, tetra- and pentapeptides containing Alanine in position 1, glutamic acid (E) or glutamine (Q) in position 2, *meso*-DAP (J) or amidated *meso*-DAP (Z) in position 3, any possible amino acids (X) in position 4, and pentapeptides containing AX dipeptides at their C-terminus (Table S1).

Seventeen monomers showing more than half of the expected *b* and *y* ions in their fragmentation spectra were
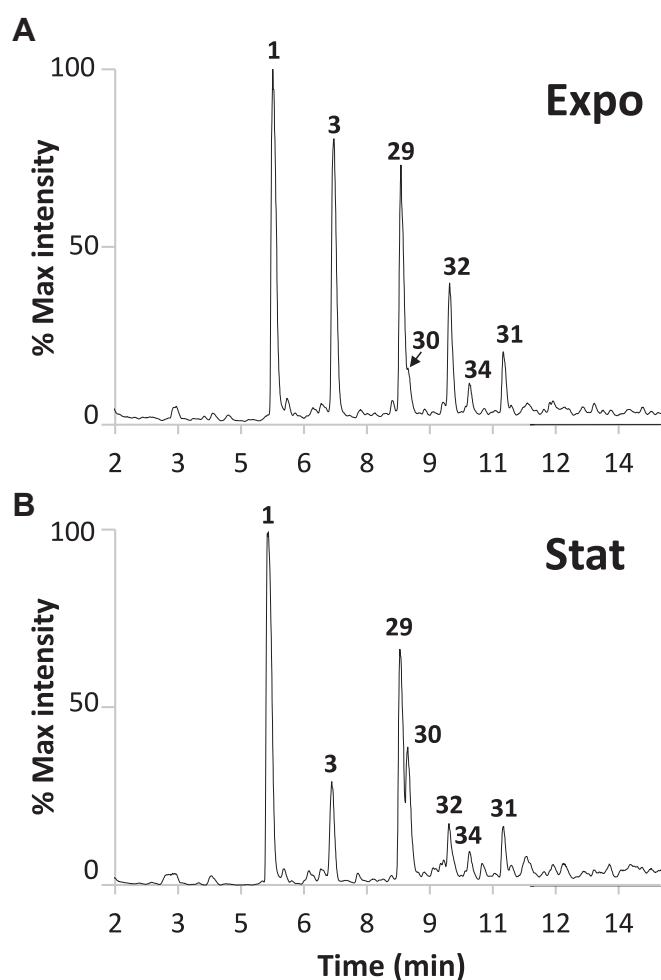

Figure 1. HPLC-MS chromatogram of *G. oxydans* reduced disaccharide-peptides. Strain B58 was grown in YPM media to exponential (*A*) or stationary phase (*B*). The numbers refer to the muropeptide structures described in Table 1.

identified by Byonic (Fig. S2). Interestingly, these included several muropeptides with a dipeptide stem other than AE that were not previously identified and a lack of tetrapeptide stems with unusual amino acids formed by canonical L,D-transpeptidases. In addition to amidated *meso*-DAP residues, we also found the presence of deacetylated *N*-acetylglucosamine residues (glucosamine) which were not previously reported. The disaccharide-peptides corresponding to these validated monomers were combined to create the database called DB0_Go (Table S2). We next performed a PGFinder search, enabling the identification of dimers and trimers with 4-3, 3-3, and 1-3 cross-links as well as modified disaccharides (deacetylated and containing MurNAc residues). A total of 61 masses matching the monoisotopic mass of theoretical structures were identified (Table 1), revealing a far more complex structure than previously reported. Peptidoglycan from cells harvested during the exponential and stationary phases showed that cross-linking index is higher in the stationary phase (19.9% *versus* 15.9%), partly due to an increased proportion of 1-3 cross-links in the stationary phase (16.6% *versus* 5.8% in exponential phase). The higher proportion of 1-3 cross-links was concomitant with the higher proportion of

Table 1
G. oxydans peptidoglycan composition

| No. | Muropeptide[a] | WT | | | | Theoretical | | |
		Expo	Stat	Ldt_{Go1}	Ldt_{Go2}	RT (min)[b]	Mass (Da)	Δppm
1	Gm-AEJ_{NH2}	36.519%	41.440%	48.001%	34.926%	5.32 ± 0.05	869.3867	4.01
2	gm-AE	4.239%	10.518%	9.628%	6.887%	6.79 ± 0.03	698.2859	2.77
3	gm-AEJA	22.572%	3.270%	4.019%	28.131%	6.80 ± 0.01	941.4018	3.38
4	gm-AE (Anh)	0.880%	1.158%	0.656%	0.505%	11.06 ± 0.00	678.2597	1.52
5	gm-AEJ_{NH2} (Anh)	0.522%	0.682%	0.472%	0.161%	8.61 ± 0.01	849.3605	2.29
6	gm-AEJ_{NH2}2A	0.254%	0.290%	0.343%	0.012%	6.37 ± 0.27	940.4238	1.39
7	gm-AEJ	0.711%	0.356%	0.193%	0.014%	5.66 ± 0.04	870.3707	2.14
8	gm-AEJAG	0.494%	0.064%	0.130%	0.247%	6.49 ± 0.02	998.4293	1.46
9	gm-AF	0.072%	0.171%	0.096%	ND	14.54 ± 0.01	716.3117	0.89
10	gm-AEJAA	0.353%	0.074%	0.094%	0.067%	8.08 ± 0.39	1012.4450	2.97
11	gm-A	0.335%	1.385%	0.534%	0.024%	6.26 ± 0.03	569.2433	1.8
12	gm-AEJA (Anh)	0.425%	0.093%	0.079%	0.131%	10.42 ± 0.01	921.3816	1.45
13	gm-AEJAK	0.114%	0.021%	0.042%	0.057%	5.86 ± 0.03	1069.5028	1.07
14	gm-AY	0.032%	0.100%	0.042%	ND	10.72 ± 0.01	732.3066	0.52
15	gm-AI	0.027%	0.070%	0.038%	ND	12.89 ± 0.00	682.3274	0.81
16	gm-AI (Anh)	ND	0.029%	ND	ND	12.75	662.3012	0.99
17	gm-AEJAR	0.121%	0.028%	0.037%	0.062%	6.42 ± 0.03	1097.5089	1.57
18	gm-AEJAH	0.100%	0.035%	0.035%	0.050%	5.99 ± 0.03	1078.4667	1.41
19	gm-AEJAN	0.022%	0.069%	0.033%	0.038%	10.37 ± 4.33	1055.4508	1.72
20	gm-AI (-Ac)	0.055%	ND	ND	ND	6.29	640.3169	0.24
21	gm-AEJ_{NH2} (-Ac)	0.036%	0.015%	0.023%	0.022%	5.05 ± 0.06	827.3762	1.15
22	gm-AQ	0.057%	0.026%	0.022%	0.047%	5.77 ± 0.04	697.3019	0.97
23	gm-AEJAE	0.029%	0.019%	0.018%	0.031%	7.29 ± 0.01	1070.4504	0.50
24	gm-AEJ (Anh)	0.011%	ND	0.017%	ND	9.03 ± 0.02	850.3445	1.15
25	gm-AEJA (-Ac)	0.021%	0.002%	0.007%	0.027%	6.43 ± 0.02	899.3973	1.11
26	gm-AEJ_{NH2}A (Anh)	ND	ND	0.006%	ND	9.93	920.3976	1.17
27	gm-AE (-Ac)	ND	0.030%	0.003%	ND	**5.62 ± 0.01**	656.2754	0.14
28	gm-AF (-Ac)	ND	ND	0.003%	ND	16.28	674.3012	1.24
29	gm-AEJ_{NH2}=gm-AEJA	13.782%	15.265%	18.938%	15.714%	8.43 ± 0.00	1792.7836	3.35
30	gm-AEJ_{NH2}=gm-A	2.592%	13.391%	7.317%	0.037%	8.60 ± 0.00	1420.6194	1.75
31	gm-AEJ_{NH2}=gm-AEJA (Anh)	3.741%	4.098%	4.220%	4.109%	10.87 ± 0.00	1772.7574	2.38
32	gm-AEJA=gm-AEJA	6.802%	2.822%	2.318%	6.976%	9.59 ± 0.00	1864.8047	2.51
33	gm-AEJ_{NH2}=gm-A (Anh)	0.243%	0.794%	0.609%	ND	11.43 ± 0.01	1400.5932	0.85
34	gm-AEJA=gm-A	2.520%	2.028%	0.512%	0.011%	10.06 ± 0.00	1492.6405	1.02
35	gm-AEJA=gm-AEJA (Anh)	0.729%	0.388%	0.199%	0.601%	12.01 ± 0.00	1844.7785	1.37
36	gm-AEJ=gm-AEJA	0.186%	0.136%	0.127%	ND	9.03 ± 0.05	1793.7676	0.68
37	gm-AEJA=gm-A (Anh)	0.317%	0.197%	0.074%	ND	12.87 ± 0.02	1472.6143	0.41
38	gm-AEJAG=gm-AEJA	0.134%	0.055%	0.049%	0.078%	9.18 ± 0.00	1921.8262	0.54
39	gm-AEJ=gm-AEJA (Anh)	0.029%	0.023%	0.034%	ND	11.46 ± 0.02	1773.7414	1.45
40	gm-AEJAG=gm-A	0.068%	0.030%	0.022%	0.013%	10.42 ± 1.48	1549.6617	3.24
41	gm-AEJ=gm-A	0.048%	0.145%	0.019%	ND	9.38 ± 0.00	1421.6034	0.94
42	gm-AEJA=gm-AEJA (Anh)	ND	0.014%	ND	ND	9.84	1844.7786	0.09
43	gm-AEJAA=gm-AEJA	0.034%	0.009%	0.016%	0.023%	9.84 ± 0.01	1935.8419	0.67
44	gm-AEJ_{NH2}A=gm-AEJA	0.007%	0.008%	0.012%	ND	9.32 ± 0.04	1863.8207	0.70
45	gm-AEJAG=gm-AEJA (Anh)	0.032%	0.014%	0.010%	0.016%	11.53 ± 0.01	1901.8000	1.14
46	gm-AEJAR=gm-AEJA	0.017%	ND	0.006%	0.007%	**9.00 ± 0.00**	2020.9058	0.32
47	gm-AEJAN=gm-AEJA	ND	ND	0.005%	0.004%	**8.76 ± 0.01**	1978.8477	0.81
48	gm-AEJ_{NH2}A=gm-AEJA (Anh)	ND	ND	0.004%	ND	11.56	1843.7945	0.37
49	gm-AEJ_{NH2}=gm-AEJA (-Ac)	0.005%	ND	0.003%	0.004%	8.18 ± 0.03	1750.7731	2.03
50	gm-AEJAH=gm-AEJA	0.013%	ND	ND	0.006%	**8.64 ± 0.00**	2001.8636	0.74
51	gm-AEJ_{NH2}A=gm-A		ND	ND	0.005%	16.44	1491.6565	0.55
52	gm-AEJAA=gm-AEJA (Anh)	0.006%	ND	0.002%	0.004%	12.12 ± 0.01	1915.8157	0.63
53	gm-AEJAG=gm-A (Anh)	0.005%	ND	0.002%	ND	**9.71 ± 2.72**	1529.6355	1.74
54	gm-AEJAR=gm-AEJA (Anh)	0.004%	ND	ND	ND	11.24	2000.8796	0.61
55	gm-AEJ_{NH2}=gm-AEJA=gm-AEJA	0.370%	0.384%	0.551%	0.554%	9.97 ± 0.00	2716.1805	0.96
56	gm-AEJ_{NH2}=gm-AEJA=gm-AEJA (Anh)	0.180%	0.196%	0.210%	0.229%	11.84 ± 0.00	2696.1543	0.78
57	gm-AEJA=gm-AEJA=gm-AEJA	0.099%	0.045%	0.119%	0.136%	10.84 ± 0.00	2788.2016	1.89
58	gm-AEJA=gm-AEJA=gm-AEJA (Anh)	0.032%	0.015%	0.024%	0.033%	12.67 ± 0.03	2768.1754	0.28
59	gm-AEJ=gm-AEJA=gm-AEJA	ND	ND	0.019%	ND	**10.59 ± 0.00**	2717.1645	1.18
60	gm-AEJ=gm-AEJA=gm-AEJA (Anh)	ND	ND	0.005%	ND	12.51	2697.1383	0.52
61	gm-AEJAG=gm-AEJA=gm-AEJA	0.005%	ND	0.004%	0.003%	10.49 ± 0.01	2845.2231	0.53

[a] g, GlcNAc; m, MurNAc; A, Alanine; E, isoglutamic acid; J, *meso*-diaminopimelic acid; J_{NH2}, amidated *meso*-diaminopimelic acid.
[b] Standard deviations in bold are determined from two values only.

disaccharide-dipeptide structures detected in the stationary phase (13.5% *versus* 5.7%). Very little variation was observed in the glycan chain length between the exponential and stationary phase (determined using the proportion of AnhydroMurNAc residues), with the average length being equal to 24 and 22 disaccharides, respectively.

By analogy with the transpeptidation reaction leading to the formation of 3-3 bonds (Fig. 2A), we hypothesized that the formation of 1-3 bonds uses muropeptides with a dipeptide stem as donor substrates (Fig. 2B). According to this hypothesis, the enzyme is predicted to form an acyl enzyme intermediate with a disaccharide-alanine.

Identification of the L,D-transpeptidase catalyzing the formation of 1-3 cross-links in G. oxydans

Interestingly, *G. oxydans* peptidoglycan does not contain any tetrapeptide stems with unusual amino acids at their C-terminus, which are characteristic of canonical L,D-
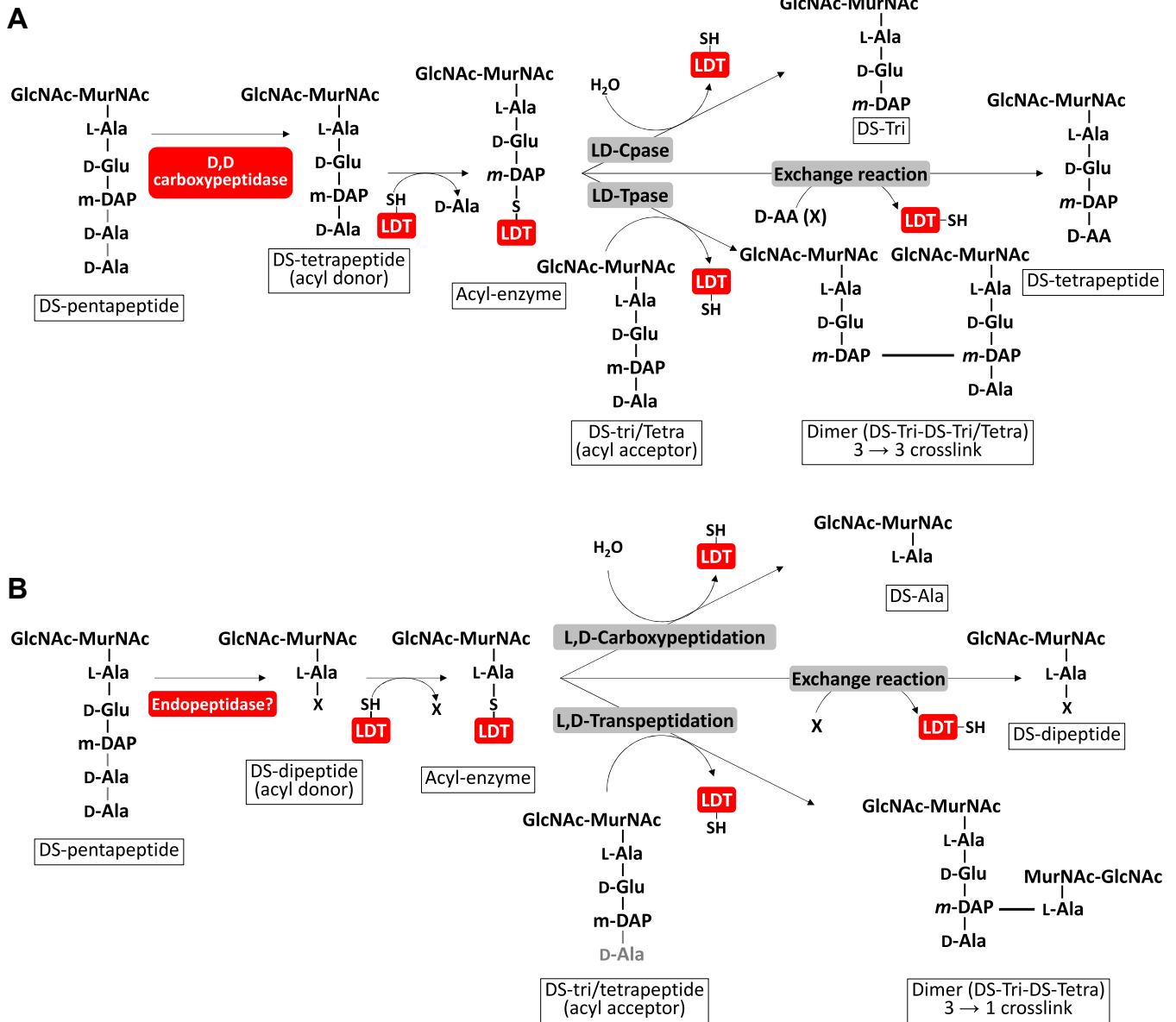
A

B

Figure 2. Schematic representation of the L,D-transpeptidation reactions leading to the formation of 3-3 and 1-3 cross-links. The enzymatic reactions carried out by L,D-transpeptidases in organisms with 3-3 cross-links are described (*A*). By analogy with these L,D transpeptidation reactions, we propose a model that leads to distinct reactions in *G. oxydans* (*B*). We hypothesize that an unidentified endopeptidase generates disaccharide dipeptides. These muropeptides are used as substrates to form an acyl-enzyme intermediate. Depending on the acceptor group, the reaction can lead to a carboxypeptidase reaction or a transpeptidation reaction that generates either a dimer or a disaccharide-dipeptide. DS, disaccharide (GlcNAc-MurNAc); DS-Tetra, disaccharide-tetrapeptide; DS-Tri, disaccharide-tripeptide; GlcNAc, *N*-acetylglucosamine; LDT, L,D-transpeptidase; MurNAc, *N*-acetylmuramic acid; X, any D amino acid.

transpeptidase enzymatic activity (Fig. 2*A*). We therefore hypothesized that in *G. oxydans*, L,D-transpeptidases could perform a similar enzymatic reaction using disaccharide-dipeptides as substrates instead (Fig. 2*B*). We searched the *G. oxydans* genome to identify genes encoding homologs of the L,D-transpeptidases and found two putative L,D-transpeptidases (labeled GOX1074, 337 residues and GOX2269, 171 residues in *G. oxydans* 621H) related to the YkuD catalytic domain (Pfam: PF03734). We hypothesized that one or both enzymes could catalyze the formation of 1-3 cross-links and renamed these putative L,D-transpeptidases Ldt$_{Go1}$ and Ldt$_{Go2}$. To test this, we took advantage of the

G. oxydans B58 Sudoku library previously described (24) and analyzed the peptidoglycan structure of the two transposon mutants with an insertion in each of the *ldt$_{Go}$* genes by LC-MS. Comparison of the total ion chromatography (TIC) profiles indicated the presence of a peak corresponding to the major 1-3 dimer (gm-AEJ$_{NH2}$=gm-A) in the wild type (Fig. 3*A*) and *ldt$_{Go1}$* mutant (Fig. 3*B*), whilst no equivalent peak was detected in the *ldt$_{Go2}$* mutant (Fig. 3*C*). Analysis of the extracted ion chromatograms for all molecules eluted between 7.5 and 11.5 min revealed a drastic reduction of 1-3 cross-links in the *ldt$_{Go2}$* peptidoglycan sample (0.035% *versus* 13.4% in the WT). The *ldt$_{Go2}$* mutation was also associated with a reduction of
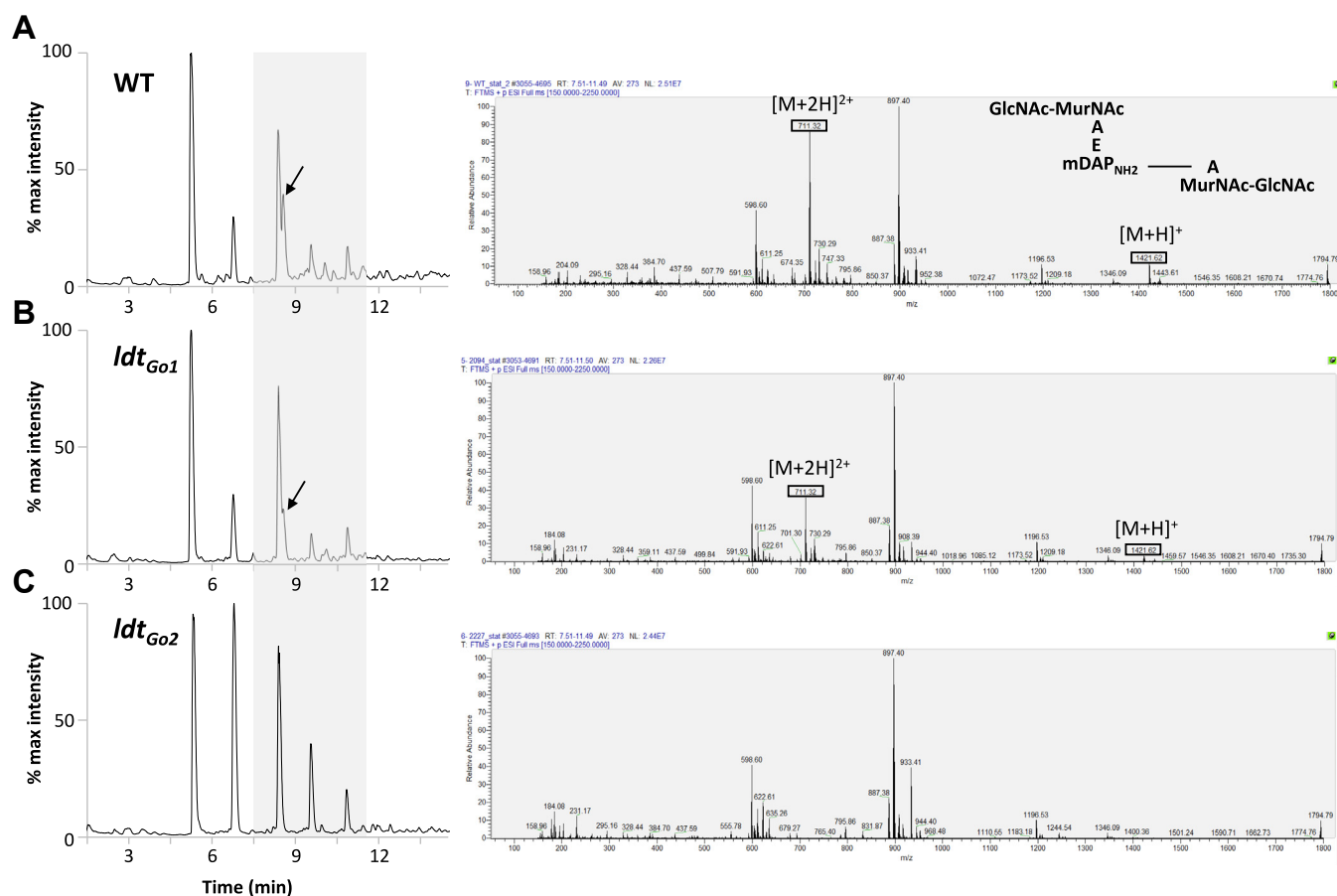
Figure 3. LC-MS detection of 1-3 2-1 cross-links in *G. oxydans* peptidoglycan. TIC of *G. oxydans* B58 (*A*) and mutants with a transposon insertion in the *ldt_{Go1}* (*B*) and *ldt_{Go2}* genes (*C*) are shown on the *left-hand side*. Extracted ions corresponding to the muropeptides eluted between 7.5 and 11.5 min are shown on the *right-hand side*. The major dimer with a 1-3 cross-link (shown with an *arrow* on the TIC and on the *top* MS spectrum) is associated with two major protonated ions: a singly charged ion with an *m/z* at 1421.32 and a doubly charged ion with an *m/z* at 711.32. None of these ions were detected in the peptidoglycan from the *ldt_{Go2}* mutant, demonstrating that this gene is essential for the formation of 1-3 cross-links.

disaccharide-dipeptides and 1-3 crosslinked dimers as compared to the parental strain and the *ldt_{Go1}* mutant (Table 1). Collectively, our LC-MS data showed that Ldt_{Go2} plays a major role in the unusual L,D-transpeptidation reactions in *G. oxydans*, including the formation of 1-3 cross-links.

Complementation and heterologous expression experiments show that the Ldt_{Go2} enzyme is sufficient to catalyse peptidoglycan 1-3 cross-links

To verify that the drastic reduction of 1-3 cross-links was associated with the disruption of *ldt_{Go2}* and not a secondary mutation, we built a complementation strain expressing Ldt_{Go2} under the anhydrotetracycline-inducible promoter (25). The production of Ldt_{Go2} in the *ldt_{Go2}* transposon mutant background clearly restored the presence of a peak corresponding to the major 1-3 cross-linked dimers (Fig. 4).

We further confirmed the enzymatic activity of Ldt_{Go2} by producing the full-length protein in *E. coli*. Since *E. coli* peptidoglycan contains disaccharide-dipeptides (gm-AE) that represent the proposed substrate for the 1-3 transpeptidation reaction, we anticipated that recombinant Ldt_{Go2} could generate the expected products found in *G. oxydans* in this

heterologous host. Peptidoglycan was purified from *E. coli* transformed with either the empty pET expression vector or a recombinant derivative expressing *ldt_{Go2}*, digested with mutanolysin, and analyzed by reverse-phase HPLC (Fig. 5A, top and bottom trace, respectively). A simple search strategy was followed to identify and quantify muropeptides resulting from unusual L,D-transpeptidation reactions (Fig. S3).

First, we identified monomers based on MS/MS data using the Byonic module from Byos. We searched for all possible disaccharide-peptides containing one to five amino acids (A, AX, AEJ, AEJX, and AEJAX, where J is *meso*-diaminopimelic acid and X any amino acid) adding sugar deacetylation previously identified in *E. coli* (23) as a potential glycan modification (Table S3). Twenty-eight monomers validated by MS/MS analysis were selected to create a database called DB0_Ec (Table S4). This monomer database was then run through PGFinder to identify, compare, and quantify muropeptides in the *E. coli* expression strain and its derivative expressing Ldt_{Go2}. To focus on 1-3 L,D transpeptidation products, we only enabled the search for 1-3 dimers that contain the gm-A moiety. Interestingly, the PGFinder search revealed a very low amount of 1-3 transpeptidation products in *E. coli* (gm-A, 0.44% and gm-AEJA=gm-A, 0.056%) (Fig. 5B). A striking
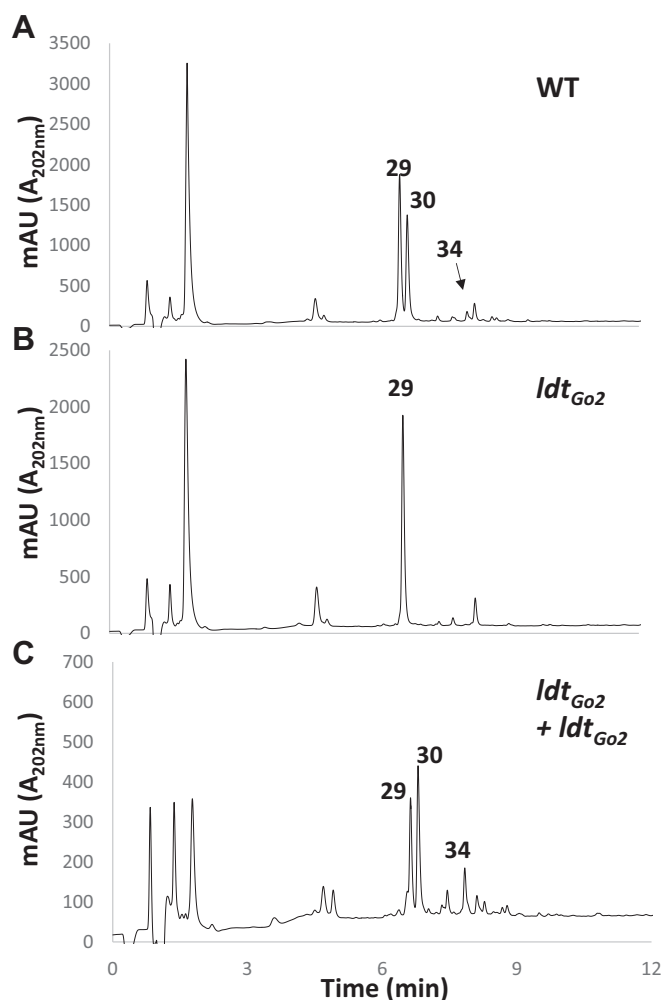
Figure 4. Complementation of the *ldt*$_{Go2}$ transposon insertion restores 1-3 cross-links. Wild-type train B58 (*A*), the *ldtGo2* insertion mutant (*B*) and the complemented mutant (*C*) were grown in YPM media. The expression of *ldt*$_{Go2}$ in the complemented strain was induced at OD$_{600nm}$ = 0.5 with 100 ng/ml anhydrotetracycline. The peaks corresponding to the major species are labelled. Numbers refer to the muropeptides described in Table 1.

increase in gm-A (9.0%), gm-AX (4.3%) monomers and dimers resulting from 1-3 cross-linking (9.5%) was detected in the peptidoglycan of the strain expressing Ldt$_{Go2}$. demonstrating that this enzyme is an L,D-transpeptidase that can perform all the reactions described in Figure 2 (carboxypeptidation, exchange, and 1-3 transpeptidation).

Ldt$_{Go2}$ is characterized by an atypical YkuD-like catalytic domain that can be found in distant families of bacteria with 1-3 peptidoglycan cross-links

To place *G. oxydans*'s L,D-transpeptidases in a broader evolutionary context, homologues were extracted from genomes of numerous alphaproteobacterial species (Table S5), including those previously shown to contain 1-3 peptidoglycan cross-links (22). Four other organisms with characterized L,D-transpeptidases (*E. coli, C. difficile, M. tuberculosis* and *E. faecium*) were added. Phylogenetic reconstruction of all putative alphaproteobacterial L,D-transpeptidases revealed

that both Ldt$_{Go1}$ and Ldt$_{Go2}$ homologues form distinct clades representing previously uncharacterised transpeptidase subfamilies (Fig. 6A).

When annotated using InterProScan and its default significance thresholds, Ldt$_{Go1}$ homologs are shown to contain a canonical YkuD (Pfam: PF03734) domain, but the more distantly related Ldt$_{Go2}$ homologs typically lack this annotation. Instead, most are annotated with a YkuD-like (CDD: cd16913) domain, and others contain no domain annotations at all (Fig. 6B). Although Ldt$_{Go2}$ is annotated with a canonical YkuD domain, it should be noted that the E-value for this annotation is high (2.0e-1), indicative of a significant divergence from the canonical YkuD domain.

Finally, to better understand the distribution of this unusual L,D-transpeptidase subfamily beyond the Alphaproteobacteria, the catalytic domain of Ldt$_{Go2}$ was searched against the entirety of the NCBI RefSeq Select database (26). Out of the 307 hits returned from unique bacterial species, roughly 37% could be attributed to *Acetobacteraceae* like *G. oxydans*, but an even greater percentage of hits (45%) came from the *Burkholderiaceae* (Fig. 6C). Though the *Acetobacteraceae* and *Burkholderiaceae* encompass the majority of Ldt$_{Go2}$ homologs, others are found sprinkled throughout the broader Burkholderiales and even beyond the Pseudomonadota, with homologs in the *Desulfovibrionaceae*. No Ldt$_{Go2}$ homologs were found in the model organisms included in our analysis (*M. tuberculosis, C. difficile, E. coli*, and *E. faecium*). Since active site geometry is thought to be a key determinant of L,D-transpeptidase substrate preference and activity, a further search for structural homologues was conducted using Foldseek and an AlphaFold model of the Ldt$_{Go2}$ catalytic domain (27, 28). Setting an E-value threshold of ≤ 2e-2 (selecting for matches better than *Bacillus subtilis*' prototypical YkuD domain), led to 147 hits. The results of this structural search largely validated the results of the sequence-based BlastP search, with 22% of hits coming from the *Acetobacteraceae* and 39% from the *Burkholderiaceae*, but a much larger number of hits (23%) now fell outside of the families found by BLAST.

Overall, these analyses establish that L,D-transpeptidases associated with 1-3 cross-linking contain a catalytic domain related to the canonical YkuD transpeptidase domain but form a distinct enzymatic subfamily.

Discussion

In this study, we determine the high-resolution structure of *G. oxydans* peptidoglycan using a version of PGFinder that can generate dynamic databases containing 1-3 cross-linked multimers. We show that *G. oxydans* peptidoglycan contains a high proportion of dipeptide stems with unusual amino acids at their C-terminus, leading us to propose that the enzyme forming 1-3 cross-links uses dipeptide stems as a donor substrate. We identify 2 *G. oxydans* enzymes distantly related to L,D-transpeptidases making 3-3 cross-links. Based on the characterization of a transposon mutant and heterologous
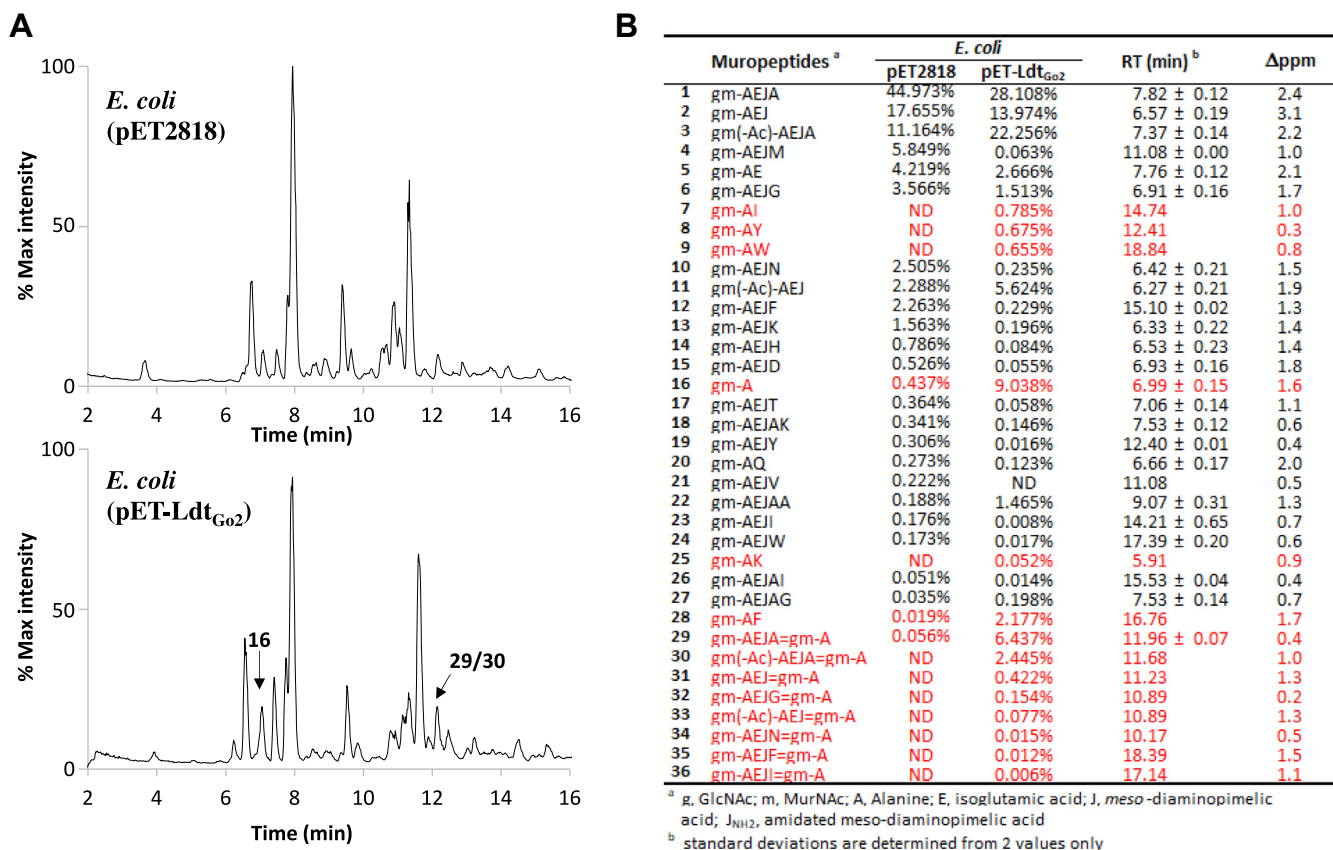
A

B

Muropeptides [a]	E. coli		RT (min) [b]	Δppm
	pET2818	pET-Ldt_{Go2}		
1 gm-AEJA	44.973%	28.108%	7.82 ± 0.12	2.4
2 gm-AEJ	17.655%	13.974%	6.57 ± 0.19	3.1
3 gm(-Ac)-AEJA	11.164%	22.256%	7.37 ± 0.14	2.2
4 gm-AEJM	5.849%	0.063%	11.08 ± 0.00	1.0
5 gm-AE	4.219%	2.666%	7.76 ± 0.12	2.1
6 gm-AEJG	3.566%	1.513%	6.91 ± 0.16	1.7
7 gm-AI	ND	0.785%	14.74	1.0
8 gm-AY	ND	0.675%	12.41	0.3
9 gm-AW	ND	0.655%	18.84	0.8
10 gm-AEJN	2.505%	0.235%	6.42 ± 0.21	1.5
11 gm(-Ac)-AEJ	2.288%	5.624%	6.27 ± 0.21	1.9
12 gm-AEJF	2.263%	0.229%	15.10 ± 0.02	1.3
13 gm-AEJK	1.563%	0.196%	6.33 ± 0.22	1.4
14 gm-AEJH	0.786%	0.084%	6.53 ± 0.23	1.4
15 gm-AEJD	0.526%	0.055%	6.93 ± 0.16	1.8
16 gm-A	0.437%	9.038%	6.99 ± 0.15	1.6
17 gm-AEJT	0.364%	0.058%	7.06 ± 0.14	1.1
18 gm-AEJAK	0.341%	0.146%	7.53 ± 0.12	0.6
19 gm-AEJY	0.306%	0.016%	12.40 ± 0.01	0.4
20 gm-AQ	0.273%	0.123%	6.66 ± 0.17	2.0
21 gm-AEJV	0.222%	ND	11.08	0.5
22 gm-AEJAA	0.188%	1.465%	9.07 ± 0.31	1.3
23 gm-AEJI	0.176%	0.008%	14.21 ± 0.65	0.7
24 gm-AEJW	0.173%	0.017%	17.39 ± 0.20	0.6
25 gm-AK	ND	0.052%	5.91	0.9
26 gm-AEJAI	0.051%	0.014%	15.53 ± 0.04	0.4
27 gm-AEJAG	0.035%	0.198%	7.53 ± 0.14	0.7
28 gm-AF	0.019%	2.177%	16.76	1.7
29 gm-AEJA=gm-A	0.056%	6.437%	11.96 ± 0.07	0.4
30 gm(-Ac)-AEJA=gm-A	ND	2.445%	11.68	1.0
31 gm-AEJ=gm-A	ND	0.422%	11.23	1.3
32 gm-AEJG=gm-A	ND	0.154%	10.89	0.2
33 gm(-Ac)-AEJ=gm-A	ND	0.077%	10.89	1.3
34 gm-AEJN=gm-A	ND	0.015%	10.17	0.5
35 gm-AEJF=gm-A	ND	0.012%	18.39	1.5
36 gm-AEJI=gm-A	ND	0.006%	17.14	1.1

[a] g, GlcNAc; m, MurNAc; A, Alanine; E, isoglutamic acid; J, *meso*-diaminopimelic acid; J_{NH2}, amidated meso-diaminopimelic acid

[b] standard deviations are determined from 2 values only

Figure 5. Heterologous protein synthesis of Ldt_{Go2} in *E. coli* BL21(DE3) increases the proportion of 1-3 L,D-transpeptidation products. *E. coli* BL21(DE3) transformed with the control pET2818 plasmid or pET2818 encoding Ldt_{Go2} was grown in auto-induction medium overnight and peptidoglycan from both cultures were purified. The muropeptide profile are shown in (*A*); *bottom* profile is from the control strain; *bottom panel* is from *E. coli* (pET-ldt_{Go2}). Two major peaks containing muropeptides of interest resulting from 1-3 L,D-transpeptidation are indicated. *B*, PGFinder analysis of *E. coli* control strain (transformed with the empty plasmid, *E. coli* (pET2818)) and expressing Ldt_{Go2} (*E. coli* (pET-Ldt_{Go2})). Only monomers validated by Byonic based on MS/MS data were search as well as their 1-3 transpeptidation products. The monomers and dimers resulting from 1-3 L,D-transpeptidation are indicated in *red*.

expression experiments, we demonstrate that one of these two candidates (Ldt_{Go2}) catalyses the formation of 1-3 cross-links.

This work demonstrated that Ldt_{Go2} plays a predominant role in the formation of 1-3 cross-links in *G. oxydans*. The role of Ldt_{Go1} remains unclear since the inactivation of the corresponding gene is associated with only marginal changes in the peptidoglycan composition (Table 1). Our attempts to express recombinant Ldt_{Go1} and Ldt_{Go2} in *E. coli* as his-tagged or maltose-binding fusion proteins remained unsuccessful and both proteins were systematically found in the insoluble fraction, irrespective of the expression strains and conditions tested. Further experiments are therefore required to produce and purify these recombinant proteins to examine their activity *in vitro* more closely.

The formation of 3-3 cross-links in Enterococci is controlled by the availability of disaccharide-tetrapeptides used as donor substrate. In *E. faecium*, L,D-transpeptidation can bypass the D,D-transpeptidation following the activation of a cryptic D,D-carboxypeptidase (29). How the disaccharide-dipeptide substrates are generated in *G. oxydans* remains unknown. *G. oxydans* encodes two potential endopeptidases containing a CHAP domain that could generate Ldt_{Go2} substrates (GOX_RS06930 and GOX_RS07380 in *G. oxydans* 621H). The transposon inactivation of each gene was tested

but did not abolish the production of 1-3 cross-links (data not shown), indicating that these genes do not play a predominant role in the formation of dipeptide stems or are functionally redundant. The inactivation of both genes simultaneously will be required to further investigate the Ldt_{Go2} partners that contribute to the formation of unusual cross-links.

Interestingly, three Ldt_{Go2} homologs, those found in *Roseomonas gilardii*, *Acidocella facilis*, and *Acidomonas methanolica*, were not annotated with any YkuD-like (CDD: cd16913) catalytic domains by InterProScan. Although 1-3 cross-links have only been reported in *A. methanolica* (22), it would be worth revisiting the peptidoglycan in the two other species to confirm the absence of 1-3 cross-links using PGFinder. This work confirms previous studies which showed that this software is a powerful tool to elucidate the high-resolution of bacterial peptidoglycan structures and their quantification. Unlike peptidoglycan analyses based on UV quantification, PGFinder allows the systematic and unbiased identification of low-abundance muropeptides accounting for less than 0.01% of all muropeptides. A striking result illustrating the low detection threshold provided by PGFinder is the identification of 1-3 crosslinks and gm-A muropeptides in *E. coli*, indicating that these organisms' L,D-transpeptidases can also form unusual reactions.
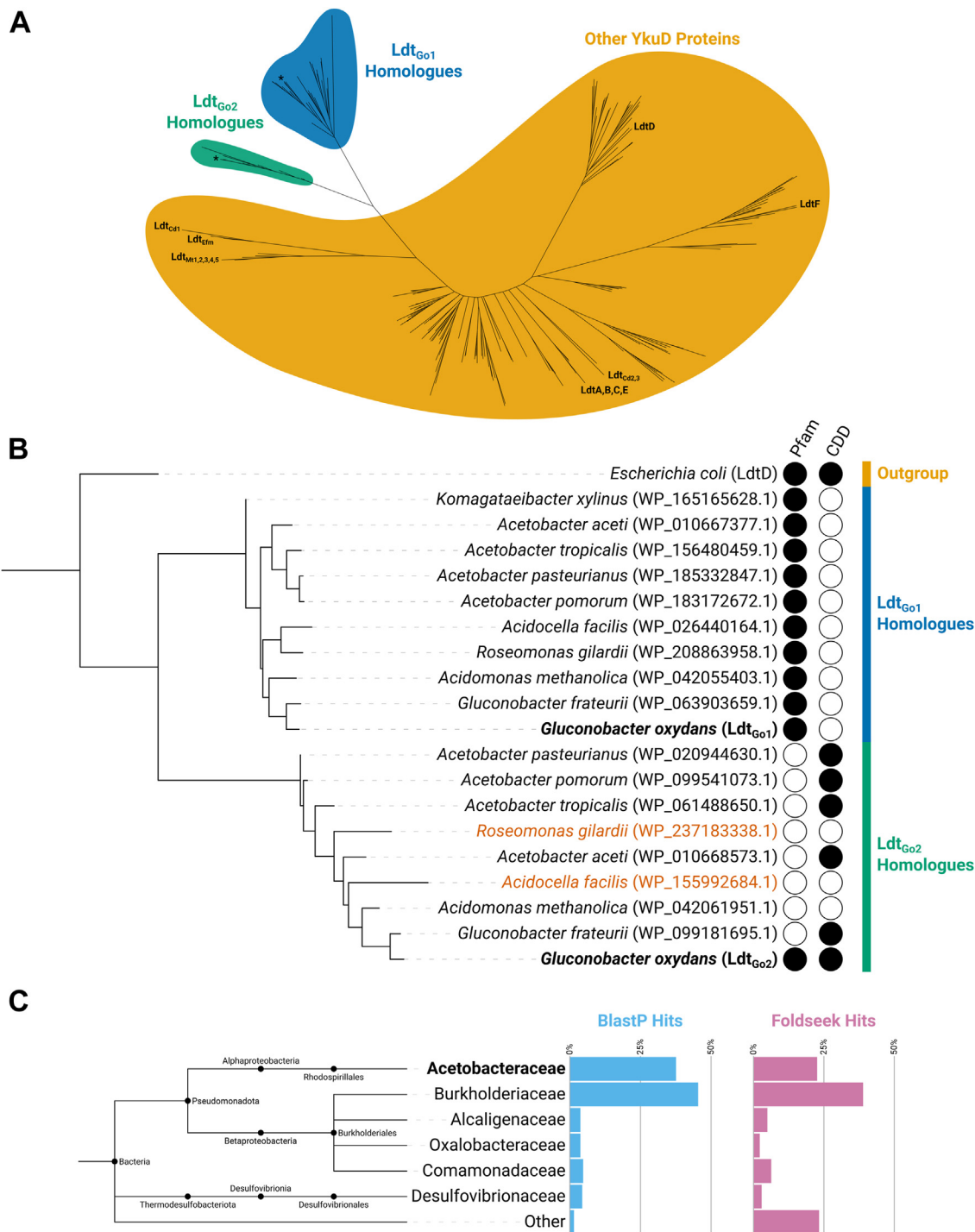
ASBMB

J. Biol. Chem. (2024) 300(1) 105494 **7**

Figure 6. Ldt$_{Go2}$ represents a distinct L,D-transpeptidase subclade with a divergent catalytic domain that is found primarily in the *Aceto-bacteraceae* and *Burkholderiaceae*. *A*, an unrooted phylogenetic tree of putative L,D-transpeptidases throughout Alphaproteobacteria and characterized enzymes (Table S5) reveals that Ldt$_{Go1}$ and Ldt$_{Go2}$ homologues form distinct transpeptidase subfamilies. Ldt$_{Go1}$ and Ldt$_{Go2}$ are labelled with asterisks (*). Previously characterised L,D-transpeptidases from *Escherichia coli* (LdtA-F), Clostridioides difficile (LdtCd1-3), *Mycobacterium tuberculosis* (LdtMt1-5) and *Enterococcus faecium* (Ldt$_{Efm}$) have also been labelled. *B*, a phylogram of Ldt$_{Go1}$, Ldt$_{Go2}$, and their homologues reveals that whilst all Ldt$_{Go1}$ homologues were annotated with the canonical L,D-transpeptidase Pfam domain (YkuD) (43), most Ldt$_{Go2}$ homologues were annotated only with the CDD YkuD_like domain (44), and the rest lacked domain annotation entirely. The Ldt$_{Go2}$ homologues highlighted in *orange* are found in bacterial species where no 1-3 cross-links could be detected (22). *C*, an expanded search for Ldt$_{Go2}$ homologues beyond the Alphaproteobacteria reveals the presence of this subfamily throughout the Burkholderiales and *Desulfovibrionaceae*. Structural homologues located using Foldseek (28) show a similar evolutionary distribution as those located using BlastP (26).

Moving from sequence to structural analysis, the predicted fold of Ldt$_{Go2}$ revealed the presence of a much more open, bowl-like active site (Fig. 7). Given that this enzyme uses a shorter peptide stem as a donor substrate, it is likely that the catalytic site does not require canonical cleft or trapping loops to accommodate the substrate. Instead, the open conformation
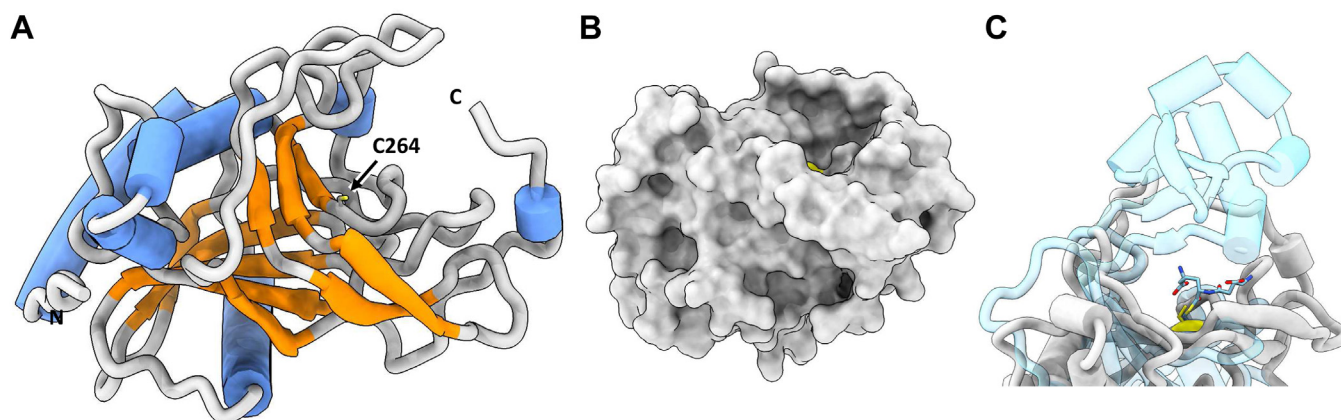
Figure 7. Structural analysis of *G. oxydans* Ldt_{Go2}. *A*, predicted fold of Ldt_{Go2}, inclusive of well-modeled residues 79 to 336, taken from EBI Alphafold repository (27). The catalytic residue (C264) shown in stick form with SH sidechain coloured *yellow*. *B*, surface representation of Ldt_{Go2}, demonstrating flat bowl-like active site surrounding C264 (*yellow*). *C*, superimposition of Ldt_{Go2} (*grey*) with *Vibrio cholerae* LdtA (RCSB entry 7AJO, unreleased, *blue*; bound reaction intermediate at C444 shown in stick form), reveals the relatively more closed/capped cleft of 3-3 cross-link forming enzymes and outlines that potential donor and acceptor substrates of Ldt_{Go2} will likely be less constrained.

of the catalytic site could ensure that the bulky sugar moieties of a dipeptide substrate don't limit access to the catalytic cysteine residue responsible for the formation of 1-3 cross-links.

The discovery of enzymes forming 1-3 cross-links reaffirmed that the catalytic reactions carried out by domains belonging to the YkuD family are very diverse. This work expands our knowledge of peptidoglycan polymerization and opens new avenues to study how remodeling contributes to the maintenance of cell envelope integrity (20). *Acetobacteraceae* (also called acetic acid bacteria) are important for the food industry and are key organisms involved in the production of vinegar (30). These organisms have a high capacity to oxidize ethanol as well as various sugars to form acetic acid and display resistance to high concentrations of acetic acid released into the fermentative medium. It is tempting to speculate that the formation of 1-3 cross-links contributes to the maintenance of cell envelope integrity in these harsh conditions.

Experimental procedures

Bacterial strains, plasmids, oligonucleotides, and growth conditions

Bacterial strains, plasmids, and oligonucleotides are described in Table S6. *G. oxydans* B58 (ATCC NRLL-BR8) and isogenic derivatives were grown in yeast peptone mannitol (YPM; 5 g/l yeast extract, 3 g/l peptone, 25 g/l mannitol) broth or agar at 30 $^{\circ}$C under agitation (200 rpm). *G. oxydans* cultures were inoculated with an overnight preculture at an OD_{600nm}=0.05 and grown for 36 h to stationary phase. *G. oxydans* transposon mutants were grown in the presence of kanamycin (100 μg/ml) and gentamicin (10 μg/ml) for complementation experiments Ldt_{Go2} expression in *G. oxydans* was induced by adding 100 ng/ml anhydrotetracycline to the media at an OD_{600nm}=0.5. For heterologous expression, *E. coli* was grown in an auto-induction medium (31) at 30 $^{\circ}$C under agitation (200 rpm) supplemented with 100 μg/ml ampicillin.

Plasmid constructions

Plasmid pBBR-TetR-Go2227 used to complement the transposon insertion in the *ldt_{Go2}* is a derivative of pBBR1MCS-5-T_{gdhM}-*tetR-mNG* allowing the inducible expression of proteins in *G. oxydans* under the control of the tetracycline promoter (25). pBBR-TetR-Go2227 was built using Golden Gate assembly. Three PCR fragments corresponding to (i) the gentamicin cassette (1632 bp), (ii) the pBBR1 origin of replication + the TetR gene (4029 bp), and (iii) the *ldt_{Go2}* full length sequence (1021 bp) were amplified using oligos SM_0729 + SM_0730, SM_0725 + SM_0726 and SM_0727 + SM_0728, respectively using pBBR1MCS-5-T_{gdhM}-*tetR-mNG* or *G. oxydans* chromosomal DNA as templates. The PCR products were purified by gel extraction, mixed in an equimolar ratio, and assembled using the NEBridge Golden Gate Assembly Kit (BsaI-HF v2) according to the manufacturer's instructions. Recombinant plasmids were screened by PCR and plasmid candidates were fully sequenced by Plasmidsaurus (Plsamidsaurus.com) to confirm the absence of mutations.

pET-Go2227, a pET2818 derivative expressing the full-length Ldt_{Go2} enzyme was built using a synthetic DNA fragment with optimized codon usage for *E. coli* provided by Genewiz. The synthetic open reading frame corresponding to the full-length Ldt_{Go2} gene (with a stop codon) was cloned into pET2818 as a NcoI-XhoI fragment.

Preparation of *G. oxydans* competent cells and transformation

G. oxydans was grown in 100 ml of YPM to an OD_{600nm} of 0.9 and spun for 10 min at 4000*g* at 4 $^{\circ}$C. After three washes in 1 mM 4-(2-hydroxyethyl)-1-piperazineethanesulfonic acid (HEPES) buffer (pH7.0), cells were resuspended in 250 μl. Electroporation was carried out in 1 mm cuvettes using 50 μl of electrocompetent cells and 100 ng of plasmid in a volume of 1-2 μl; parameters for electroporation were 2 kV, 25 μF and 200 Ω. After the pulse, 800 μl of YPM media supplemented with 0.25% (m/v) $MgSO_4$ and 0.15% (m/v) $CaCl_2$ was added to

the cells that were left to recover under agitation for 16 h before plating on YPM media supplemented with kanamycin and gentamicin.

Peptidoglycan extraction

G. oxydans and *E. coli* strains were grown until the stationary phase in YPM or auto-induction medium, respectively. Cells were pelleted, supernatant discarded, and cell pellet snap frozen in liquid nitrogen. The cell pellet was resuspended in 20 ml of boiling MilliQ water (MQ) before the addition of sodium dodecyl sulfate (SDS) at a final concentration of 4% (m/v). After 30 min at 100 °C, the cells were cooled down to room temperature. Peptidoglycan was pelleted at 150,000*g* for 1 h, washed five times using warm MQ water, freeze-dried and resuspended at a final concentration of 10 mg/ml.

Preparation of soluble muropeptides

2 mg of purified peptidoglycan was digested for 16 h in 20 mM phosphate buffer (pH 5.5) supplemented with 250 Units of mutanolysin (Sigma) in a final volume of 200 μl. Following heat inactivation of mutanolysin (5 min at 100 °C), soluble disaccharide peptides were mixed with an equal volume of 250 mM borate buffer (pH 9.25) and reduced with 0.2% (m/v) sodium borohydride. After 20 min at room temperature, the pH was adjusted to 5.0 using phosphoric acid. Reduced muropeptides were analyzed by HPLC using a C18 analytical column (Hypersil Gold aQ, 1.9 μm particles, 150 × 2.1 mm; Thermo Fisher Scientific) at a temperature of 50 °C. Muropeptide elution was performed at 0.3 ml/min by applying a mixture of solvent A (water, 0.1% [v/v] formic acid) and solvent B (acetonitrile, 0.1% [v/v] formic acid). LC conditions were 0 to 12.5% B for 25 min increasing to 20% B for 10 min. After 5 min at 95%, the column was re-equilibrated for 10 min with 100% buffer A. UV absorbance at 202 nm was used to check the quality of samples and determine the volume to inject for LC-MS. A volume of sample with an intensity of the most abundant monomer of 1500 mAU was used, giving an ion intensity of approximately 5.10^9.

LC-MS/MS

An Ultimate 3000 High-Performance Liquid Chromatography (HPLC; Dionex/Thermo Fisher Scientific) system coupled with a high-resolution Orbitrap Exploris 240 mass spectrometer (Thermo Fisher Scientific) was used for LC-MS analysis. Muropeptides were separated using a C18 analytical column (Hypersil Gold aQ, 1.9 μm particles, 150 × 2.1 mm; Thermo Fisher Scientific) at a temperature of 50 °C. Muropeptide elution was performed as described in the previous paragraph. The Orbitrap Exploris 240 was operated under electrospray ionization (H-ESI high flow)-positive mode, full scan (*m/z* 150–2250) at resolution 120,000 (FWHM) at *m/z* 200, with normalized AGC Target 100%, and automated maximum ion injection time (IT). Data-dependent MS/MS were acquired on a 'Top 5' data-dependent mode using the following parameters: resolution 30,000; AGC 100%, automated IT, with normalized collision energy 25%.

Analysis of peptidoglycan structure

LC-MS datasets were deconvoluted with the Byos software v3.11 (Protein Metrics). Sequential searches were carried out with PGFinder v1.1.1, with default settings (10 ppm tolerance, 0.5 min cleanup window) following the strategy described in Figs. S1 and S3. Data from individual matching output was consolidated as previously described to calculate average intensities, retention times, observed monoisotopic masses, and ppm differences. The output from individual searches and consolidated data are described in Files S1 and S2). Cross-linking index and glycan chain length were determined as described previously (32). The cross-linking index is defined as 0.5 * (% of dimers) + 0.33 * (% of trimers); glycan chain length was inferred from the abundance of anhydroMurNAc groups, which are found at the end of glycan chains. It is defined as 1/(% of AnhydroMurNAc monomers + 0.5 * (% of AnhydroMurNAc dimers) + 0.33 * (% of AnhydroMurNAc trimers).

Comparative genomics and bioinformatic analysis

Reference genomes and protein sequences (Table S5) were downloaded from NCBI Datasets (v15.25.0), and protein sequences were annotated locally using InterProScan (v5.64-96.0) (33, 34). A custom Julia (35) script was then used to search the produced GFF3 files for YkuD-containing proteins and to extract their catalytic domains. Ldt_{Go1} and Ldt_{Go2} homologues were located by running a PSI-BLAST on the RefSeq Select database restricted to taxa in (Table S5) and iterating until no new hits were returned (26). Extracted YkuD proteins and $Ldt_{Go1/2}$ homologues were aligned using Muscle (v5.1) (36), and maximum likelihood trees were constructed using IQ-TREE (v2.2.2.7) with ModelFinder (which selected WAG+R7 for Fig. 6*A* and WAG + F + G4 for Fig. 6*B*) and 1000 UFBoot replicates enabled (37–39). Trees were visualised and annotated using iTOL (v6.8.1) (40) with finishing touches applied in Inkscape (v1.3). ColabFold's AlphaFold2_batch notebook (v1.5.2) was used with the default settings and relaxation enabled to obtain predicted structures for Ldt_{Go1}, Ldt_{Go2}, and their respective catalytic domains (27, 41). Finally, Foldseek (v8-ef4e960) was used to search the AFDB50 database for structural homologues of Ldt_{Go2} (27, 42).

Data availability

LC-MS/MS datasets have been deposited in the GLYCO-POST repository (GPST000377). All plasmid sequences are available upon request. *G. oxydans* NRRL B58 genome has been deposited at DDBJ/ENA/GenBank under the accession JAIPVW000000000.

Code availability

The script for PGFinder v1.1.0 is available at https://github.com/Mesnage-Org.

Conflict of interest—The authors declare that they have no conflicts of interest with the contents of this article.

Abbreviations—The abbreviations used are: DAP, diaminopimelic acid; HEPES, 4-(2-hydroxyethyl)-1-piperazineethanesulfonic acid; MQ, MilliQ water; MS/MS, tandem mass spectrometry; MurNAC, *N*-acetylmuramic acid; PBP, Penicillin Binding Protein; SDS, sodium dodecyl sulfate; TIC, Total Ion Chromatograms; YPM, yeast peptone mannitol.

References

1. Weidel, W., and Pelzer, H. (1964) Bagshaped macromolecules - a new outlook on bacterial cell walls. *Adv. Enzymol. Relat. Subj. Biochem.* **26**, 193–232
2. Vollmer, W., Blanot, D., and de Pedro, M. A. (2008) Peptidoglycan structure and architecture. *FEMS Microbiol. Rev.* **32**, 149–167
3. Ciak, J., and Hahn, F. E. (1957) Penicillin-induced lysis of *Escherichia coli. Science* **125**, 119–120
4. Park, J. T., and Strominger, J. L. (1957) Mode of action of penicillin. *Science* **125**, 99–101
5. Tipper, D. J., and Strominger, J. L. (1965) Mechanism of action of penicillins: a proposal based on their structural similarity to acyl-D-alanyl-D-alanine. *Proc. Natl. Acad. Sci. U. S. A.* **54**, 1133–1141
6. Cho, H., Uehara, T., and Bernhardt, T. G. (2014) Beta-lactam antibiotics induce a lethal malfunctioning of the bacterial cell wall synthesis machinery. *Cell* **159**, 1300–1311
7. Wietzerbin, J., Das, B. C., Petit, J. F., Lederer, E., Leyh-Bouille, M., and Ghuysen, J. M. (1974) Occurrence of D-alanyl-(D)-meso-diaminopimelic acid and meso-diaminopimelyl-meso-diaminopimelic acid interpeptide linkages in the peptidoglycan of Mycobacteria. *Biochemistry* **13**, 3471–3476
8. Lavollay, M., Arthur, M., Fourgeaud, M., Dubost, L., Marie, A., Veziris, N., *et al.* (2008) The peptidoglycan of stationary-phase *Mycobacterium tuberculosis* predominantly contains cross-links generated by L,D-transpeptidation. *J. Bacteriol.* **190**, 4360–4366
9. Mahapatra, S., Crick, D. C., McNeil, M. R., and Brennan, P. J. (2008) Unique structural features of the peptidoglycan of *Mycobacterium leprae. J. Bacteriol.* **190**, 655–661
10. Peltier, J., Courtin, P., El Meouche, I., Lemee, L., Chapot-Chartier, M. P., and Pons, J. L. (2011) *Clostridium difficile* has an original peptidoglycan structure with a high level of N-acetylglucosamine deacetylation and mainly 3-3 cross-links. *J. Biol. Chem.* **286**, 29053–29062
11. Mainardi, J. L., Fourgeaud, M., Hugonnet, J. E., Dubost, L., Brouard, J. P., Ouazzani, J., *et al.* (2005) A novel peptidoglycan cross-linking enzyme for a beta-lactam-resistant transpeptidation pathway. *J. Biol. Chem.* **280**, 38146–38152
12. Kim, H. S., Im, H. N., An, D. R., Yoon, J. Y., Jang, J. Y., Mobashery, S., *et al.* (2015) The cell shape-determining Csd6 protein from *Helicobacter pylori* constitutes a new family of L,D-Carboxypeptidase. *J. Biol. Chem.* **290**, 25103–25117
13. Godessart, P., Lannoy, A., Dieu, M., Van der Verren, S. E., Soumillion, P., Collet, J. F., *et al.* (2021) beta-Barrels covalently link peptidoglycan and the outer membrane in the alpha-proteobacterium *Brucella abortus. Nat. Microbiol.* **6**, 27–33
14. Sandoz, K. M., Moore, R. A., Beare, P. A., Patel, A. V., Smith, R. E., Bern, M., *et al.* (2021) beta-Barrel proteins tether the outer membrane in many Gram-negative bacteria. *Nat. Microbiol.* **6**, 19–26
15. Bahadur, R., Chodisetti, P. K., and Reddy, M. (2021) Cleavage of Braun's lipoprotein Lpp from the bacterial peptidoglycan by a paralog of l,d-transpeptidases, LdtF. *Proc. Natl. Acad. Sci. U. S. A.* **118**, e2101989118
16. Galley, N. F., Greetham, D., Alamán-Zárate, M. G., Williamson, M. P., Evans, C. A., Spittal, W. D., *et al.* (2023) *Clostridioides difficile* canonical L,D-transpeptidases catalyse a novel type of peptidoglycan cross-links and are not required for beta-lactam resistance. *J. Biol. Chem.*, 105529
17. Winkle, M., Hernandez-Rocamora, V. M., Pullela, K., Goodall, E. C. A., Martorana, A. M., Gray, J., *et al.* (2021) DpaA detaches braun's lipoprotein from peptidoglycan. *mBio* **12**, e00836-00821
18. Bern, M., Beniston, R., and Mesnage, S. (2017) Towards an automated analysis of bacterial peptidoglycan structure. *Anal. Bioanal. Chem.* **409**, 551–560
19. Sutterlin, L., Edoo, Z., Hugonnet, J. E., Mainardi, J. L., and Arthur, M. (2018) Peptidoglycan cross-linking activity of L,D-Transpeptidases from *Clostridium difficile* and inactivation of these enzymes by beta-lactams. *Antimicrob. Agents Chemother.* **62**, e01607–01617
20. More, N., Martorana, A. M., Biboy, J., Otten, C., Winkle, M., Serrano, C. K. G., *et al.* (2019) Peptidoglycan remodeling enables *Escherichia coli* to survive severe outer membrane assembly defect. *mBio* **10**, e02729-18
21. Hernandez, S. B., Castanheira, S., Pucciarelli, M. G., Cestero, J. J., Rico-Perez, G., Paradela, A., *et al.* (2022) Peptidoglycan editing in non-proliferating intracellular *Salmonella* as source of interference with immune signaling. *PLoS Pathog.* **18**, e1010241
22. Espaillat, A., Forsmo, O., El Biari, K., Bjork, R., Lemaitre, B., Trygg, J., *et al.* (2016) Chemometric analysis of bacterial peptidoglycan reveals atypical modifications that empower the cell wall against predatory enzymes and fly innate immunity. *J. Am. Chem. Soc.* **138**, 9193–9204
23. Patel, A. V., Turner, R. D., Rifflet, A., Acosta-Martin, A. E., Nichols, A., Awad, M. M., *et al.* (2021) PGFinder, a novel analysis pipeline for the consistent, reproducible, and high-resolution structural analysis of bacterial peptidoglycans. *Elife* **10**, e70597
24. Schmitz, A. M., Pian, B., Medin, S., Reid, M. C., Wu, M., Gazel, E., *et al.* (2021) Generation of a *Gluconobacter oxydans* knockout collection for improved extraction of rare earth elements. *Nat. Commun.* **12**, 6693
25. Fricke, P. M., Lurkens, M., Hunnefeld, M., Sonntag, C. K., Bott, M., Davari, M. D., *et al.* (2021) Highly tunable TetR-dependent target gene expression in the acetic acid bacterium *Gluconobacter oxydans. Appl. Microbiol. Biotechnol.* **105**, 6835–6852
26. Camacho, C., Coulouris, G., Avagyan, V., Ma, N., Papadopoulos, J., Bealer, K., *et al.* (2009) BLAST+: architecture and applications. *BMC Bioinformatics* **10**, 421
27. Jumper, J., Evans, R., Pritzel, A., Green, T., Figurnov, M., Ronneberger, O., *et al.* (2021) Highly accurate protein structure prediction with AlphaFold. *Nature* **596**, 583–589
28. van Kempen, M., Kim, S. S., Tumescheit, C., Mirdita, M., Lee, J., Gilchrist, C. L. M., *et al.* (2023) Fast and accurate protein structure search

with Foldseek. *Nat. Biotechnol.* https://doi.org/10.1038/s41587-023-01773-0

29. Sacco, E., Hugonnet, J. E., Josseaume, N., Cremniter, J., Dubost, L., Marie, A., *et al.* (2010) Activation of the L,D-transpeptidation peptidoglycan cross-linking pathway by a metallo-D,D-carboxypeptidase in *Enterococcus faecium. Mol. Microbiol.* **75**, 874–885

30. Gomes, R. J., Borges, M. F., Rosa, M. F., Castro-Gomez, R. J. H., and Spinosa, W. A. (2018) Acetic acid bacteria in the food industry: systematics, characteristics and applications. *Food Technol. Biotechnol.* **56**, 139–151

31. Studier, F. W. (2018) T7 expression systems for inducible production of proteins from cloned genes in *Escherichia coli. Curr. Protoc. Mol. Biol.* **124**, e63

32. Glauner, B. (1988) Separation and quantification of muropeptides with high-performance liquid chromatography. *Anal. Biochem.* **172**, 451–464

33. Blum, M., Chang, H. Y., Chuguransky, S., Grego, T., Kandasaamy, S., Mitchell, A., *et al.* (2021) The InterPro protein families and domains database: 20 years on. *Nucleic Acids Res.* **49**, D344–D354

34. Jones, P., Binns, D., Chang, H. Y., Fraser, M., Li, W., McAnulla, C., *et al.* (2014) InterProScan 5: genome-scale protein function classification. *Bioinformatics* **30**, 1236–1240

35. Bezanson, J., Edelman, A., Karpinski, S., and Shah, V. B. (2017) Julia: a fresh approach to numerical computing. *SIAM Rev.* **59**, 65–98

36. Edgar, R. C. (2004) MUSCLE: multiple sequence alignment with high accuracy and high throughput. *Nucleic Acids Res.* **32**, 1792–1797

37. Hoang, D. T., Chernomor, O., von Haeseler, A., Minh, B. Q., and Vinh, L. S. (2018) UFBoot2: improving the ultrafast bootstrap approximation. *Mol. Biol. Evol.* **35**, 518–522

38. Kalyaanamoorthy, S., Minh, B. Q., Wong, T. K. F., von Haeseler, A., and Jermiin, L. S. (2017) ModelFinder: fast model selection for accurate phylogenetic estimates. *Nat. Methods* **14**, 587–589

39. Minh, B. Q., Schmidt, H. A., Chernomor, O., Schrempf, D., Woodhams, M. D., von Haeseler, A., *et al* (2020) IQ-TREE 2: new models and efficient methods for phylogenetic inference in the genomic era. *Mol. Biol. Evol.* **37**, 1530–1534

40. Letunic, I., and Bork, P. (2021) Interactive Tree of Life (iTOL) v5: an online tool for phylogenetic tree display and annotation. *Nucleic Acids Res.* **49**, W293–W296

41. Mirdita, M., Schutze, K., Moriwaki, Y., Heo, L., Ovchinnikov, S., and Steinegger, M. (2022) ColabFold: making protein folding accessible to all. *Nat. Methods* **19**, 679–682

42. Varadi, M., Anyango, S., Deshpande, M., Nair, S., Natassia, C., Yordanova, G., *et al.* (2022) AlphaFold Protein Structure Database: massively expanding the structural coverage of protein-sequence space with high-accuracy models. *Nucleic Acids Res.* **50**, D439–D444

43. Mistry, J., Chuguransky, S., Williams, L., Qureshi, M., Salazar, G. A., Sonnhammer, E. L. L., *et al.* (2021) Pfam: the protein families database in 2021. *Nucleic Acids Res.* **49**, D412–D419

44. Wang, J., Chitsaz, F., Derbyshire, M. K., Gonzales, N. R., Gwadz, M., Lu, S., *et al.* (2023) The conserved domain database in 2023. *Nucleic Acids Res.* **51**, D384–D388